

Equilibrium and Nonequilibrium Quantum Correlations Between Two Accelerated Detectors

He Wang

*College of Physics, Jilin University,
Changchun 130021, China and*

*State Key Laboratory of Electroanalytical Chemistry,
Changchun Institute of Applied Chemistry,
Changchun 130021, China.*

Jin Wang*

*Department of Chemistry and of Physics and Astronomy,
Stony Brook University, Stony Brook,
NY 11794-3400, USA*

(Dated: June 3, 2022)

Despite the efforts, it is still challenging to quantify the quantum correlations in the curved space time. It has long been realized that the effect of the local acceleration is equivalent to a thermal temperature bath termed as Unruh effect. The two accelerated observers can detect quantum correlations between them through the vacuum field. A natural question arises: Can we quantify the quantum correlations between the two accelerated detectors or equivalently between two locations in curved space time and are these equilibrium (equal accelerations of the two detectors) quantum correlation equivalent to the ones between the two stationary detectors under a thermal bath? A further question is what if the two accelerations or the couplings between the detectors and the vacuum field are different and how this nonequilibrium effect can influence the quantum correlations. In this study, we examine the above scenarios. We found that quantum correlation harvesting from field is universal in many cases. The temperature and acceleration characterizing the equivalently effective local space-time curvature show qualitatively similar and quantitatively different impacts on the quantum correlations in this equilibrium (equal temperatures or accelerations of the two detectors) scenario. This shows the similarities and differences between the two detectors under equal accelerations or equivalently local curvatures and the same temperatures for the effects on the quantum correlations. As the acceleration (temperature) of the detectors increases, the entanglement decreases to zero at some instant but the mutual information (discord) is amplified. As the acceleration increases when the equal acceleration is in the opposite direction, the quantum correlation decays. Importantly, we show that the larger quantum correlations can appear due to the nonequilibriumness characterized by the degree of the detailed balance breaking from enhanced difference in the couplings. We also uncovered that both the nonequilibriumness (different accelerations of the two detectors or equivalently different local space time curvatures) and the distance between the detectors affect the quantum correlations between the detectors.

I. INTRODUCTION

Quantum information science has remarkable progress in the last three decades [1] and promises even more revolutionary advances in the next decades. Quantum information is often characterized by certain quantum correlation measures such as entanglement, mutual information, discord etc. Entanglement has been thought to be responsible for the spooky action over distance with quantum non-locality [2]. It is a key resource in quantum computation and information which has been studied intensively [3]. It was shown that entanglement has the pure quantum natures leading to an advantage over classical computation. Quantum mutual information is a generalization of the classical mutual information characterizing the quantum correlations between the two systems [4]. The quantum discord is the non-classical part

of the correlations characterized by the difference between the quantum mutual information and classical correlation [5].

It is worthwhile noticing that most of the studies on quantum information and quantum correlation studies concentrate on the cases when the space-time is flat. In early universe, cosmology and astrophysics, the curved space-time is unavoidable and needs to be seriously considered. [6–12]. However, the quantification of quantum correlations in the curved space time is still challenging. Furthermore, how the quantum correlations are influenced by the environment is also not so clear in curved space time. To understand the quantum information and correlations in curved space time, we can start with a simple example, the accelerated detectors. It has long been realized that the effect of the local acceleration or the related curved space-time is equivalent to a thermal temperature bath, termed as Unruh effect or Hawking effect [13, 14]. Therefore, a natural question arises: Can we quantify the quantum correlations

* jin.wang.1@stonybrook.edu

between the two accelerated detectors or between the two locations in curved space time? Are the equilibrium (same accelerations of the two detectors) quantum correlations between the two accelerated detectors or two locations of the curved space-time equivalent to the two stationary detectors under the thermal temperature bath in flat space-times? Moreover, what if the two accelerations (or the related curvatures of the space-times) or the couplings between the detectors and the vacuum field are different and how this nonequilibrium effect can influence the quantum correlations.

Quantum field theory (QFT) born from the marriage of the special relativity and the quantum mechanics [15] is suitable for studying the relativistic quantum information process. Some studies explored the entanglement between the field modes. It was shown that entanglement is observer-dependent and degraded from the perspective of the observers in uniform acceleration due to the Unruh effect. [6–8, 16] As the researchers become more interested in the entanglement or quantum correlations between the observers, particle detector models, such as the Unruh-Dewitt models, were used to show the entanglement harvesting from the coupling of the detectors to a vacuum state of a quantum field [11, 12, 17–20]. The detector is usually made of a qubit and has been shown to be useful for investigating the quantum correlations between the detectors. [11, 12, 20] There have also been approaches replacing the qubit by a harmonic oscillator to serve as the detector more realistically and computing the quantum correlations between the detectors through solving the Heisenberg equations of motion at different settings. [21, 22] Furthermore, a method was developed by Eric G. Brown et al. [23] to solve the time evolution of the particle detection for the accelerated detectors with a time dependent quadratic Hamiltonian under arbitrary number of modes in a stationary cavity. The method has the advantage of gaining the time trajectories of an arbitrary number of detectors coupled to the vacuum field in the cavity without the need of the usual Bogoliubov transformation. By replacing a qubit (two energy levels) with an harmonic oscillator (infinite energy levels) in the detector model, one gains significant advantages over the standard Unruh-DeWitt (qubit-based) detector including the practical particle detection and non-perturbative treatment [23]. Therefore, the quantum evolution of the particle detection can be solved nonperturbatively by using the symplectic formalism for Gaussian states and operations. [23] The evolution of the particle detection can then be obtained by solving (in general numerically) a set of coupled first order ordinary differential equations. This formalism is especially useful for scenarios of interest in relativistic quantum theory involving quadratic Hamiltonians. However, neither the quantum correlations of the two equally accelerated observers and their comparisons to the corresponding stationary detectors under the common thermal temperature bath nor the quantum correlations of the two different accelerated observers and their comparisons to the corresponding stationary detec-

tors under two different thermal temperature baths has been fully explored.

In this study, we consider two accelerated detectors moving inside a stationary cavity in flat space time. The detectors themselves are often considered effectively surrounded by two thermal bathes associated with Unruh temperature $T = a/2\pi$ where a is the proper acceleration of the detector. [13] We found that the dynamics of the quantum correlations between the two equally accelerated detectors in the vacuum or of the two stationary detectors in a thermal field with the temperature T have similar qualitative trend but with quantitative difference. This shows the similarities and differences between the two detectors under equal accelerations or equivalently local curvatures and the same temperatures for the effects on the quantum correlations. As the acceleration or the related local curvature (temperature) of the detectors increases, the entanglement gradually disappears, while the mutual information and the quantum discord are amplified as suggested before [24]. This shows that the quantum mutual information and discord are more robust on the environmental (field) temperature fluctuations than the entanglement. As the acceleration increases when the equal acceleration is in the opposite direction, the quantum correlations decay. This shows that the distance effect dominates the evolution.

In the meanwhile, we study the quantum correlations in the nonequilibrium scenarios where the nonequilibriumness is characterized by the degree of the detailed balance breaking due to the different couplings of the two equally accelerated detectors to the vacuum field. We show that the nonequilibriumness can enhance the quantum correlations. Another nonequilibrium scenario we consider is when the two detectors are under different accelerations mimicking the situations of different effective local temperatures. This leads to both nonequilibrium effect from the difference in accelerations and the distance effect on the quantum correlations between the two detectors.

Our paper is organized as follows. In Sec. II we review the continuous-variable techniques introduced in Ref. [23] which holds for an arbitrary time dependent quadratic Hamiltonian and an arbitrary number of modes in a stationary cavity. Based on this, we also quantify the correlation measures (the logarithmic negativity as a measure of the entanglement, the mutual information, and the Gaussian quantum discord) between the two detectors. In Sec. III we will present our main results. We have considered different scenarios for the two detectors: both stationary, both accelerated, accelerated in the same direction and opposing direction, equilibrium detectors with equal accelerations and nonequilibrium detectors with different accelerations or different couplings to the vacuum field under the same accelerations. We provided detailed discussions. In Sec. IV we give the conclusion.

II. THE MODEL

A. Time evolution of the operators

Let us consider the global Hamiltonian and discuss how the dynamics evolve with respect to the proper time of an arbitrary detector. Throughout this paper we will use the conventions with $\hbar = c = G = k_B = 1$. Consider a general time dependent Hamiltonian $\hat{H}(t)$, where t is the global time coordinate. The Heisenberg equation of motion of a general operator $\hat{A}(t)$ is then given by

$$\frac{d\hat{A}(t)}{dt} = i[\hat{H}(t), \hat{A}(t)] + \frac{\partial\hat{A}(t)}{\partial t}. \quad (1)$$

Another coordinate choice is the local proper time τ_j which corresponds to the world line $(t(\tau_j), x(\tau_j))$ traversed by the detector j at x and t . Applying the chain rule, the two time coordinates are associated,

$$\begin{aligned} \frac{d\hat{A}[t(\tau_j)]}{d\tau_j} &= \frac{dt(\tau_j)}{d\tau_j} \frac{d}{dt} \hat{A}(t)|_{t=t(\tau_j)} \\ &= \frac{dt(\tau_j)}{d\tau_j} (i[\hat{H}(t), \hat{A}(t)] + \frac{\partial\hat{A}(t)}{\partial t}) \\ &= i[\frac{dt}{d\tau_j} \hat{H}(t), \hat{A}(t(\tau_j))] + \frac{\partial\hat{A}(t(\tau_j))}{\partial\tau_j}. \end{aligned} \quad (2)$$

We can rewrite the Hamiltonian as

$$\hat{H}_j(\tau_j) = \frac{dt}{d\tau_j} \hat{H}(t(\tau_j)) \quad (3)$$

This is the Hamiltonian seen by j th detector. Therefore, we can provide a table for transformation to any other time coordinate. In fact $\frac{dt}{d\tau_j}$ is the redshift factor for an observer in the detector's reference frame. It provides an overall scaling of all energies in the whole system since this is what such an observer would experience. For the corresponding form in proper time, let us define

$$\hat{A}_j(\tau_j) = \hat{A}(t(\tau_j)) \quad (4)$$

We can use Eq.(3) and Eq.(4) to rewrite Eq.(2) for the evolution dynamics of the operator in proper time as

$$\frac{d}{d\tau_j} \hat{A}_j(\tau_j) = i[\hat{H}_j(\tau_j), \hat{A}_j(\tau_j)] + \frac{\partial\hat{A}_j(\tau_j)}{\partial\tau_j} \quad (5)$$

B. Hamiltonian of the detector, field and detector-field interactions

We will study the interactions of a number of particle detectors coupled to a quantum massless scalar field.

Let us consider an $X - X$ coupling form of the Unruh-DeWitt Hamiltonian. [11–13] A general form of the Unruh-DeWitt detector field interaction is given by

$$\hat{H}_1 = \lambda(\tau) \hat{\mu} \hat{\phi}[x(\tau_j)] \quad (6)$$

where $\lambda(\tau)$ is the switching function or coupling, $\hat{\mu}$ is the monopole moment of the detector and $\hat{\phi}[x(\tau_j)]$ is the scalar field operator evolving along the worldline of the detector parametrized in terms of the proper time τ . Here, the subscript “1” of the Hamiltonian represents the interaction term and the subscript “0” of the Hamiltonian represents the free Hamiltonian term. To derive the correct form of the Hamiltonian in the Heisenberg picture, let us first write the field and monopole operators in the Schrödinger picture. For clarity, we first consider just one detector undergoing general motion in flat space time with an associated proper time τ with a scalar quantum field expanded in terms of the plane wave solutions:

$$\hat{\phi}^S[x(\tau)] = \sum_n \hat{a}_n v_n[x(\tau)] + \hat{a}_n^\dagger v_n[x(\tau)] \quad (7)$$

Here, the superscript “S” denotes the Schrödinger picture. “H” denotes the Heisenberg picture. \hat{a}_n and \hat{a}_n^\dagger are the annihilation and the creation operator for the n th field mode respectively. v_n is the spatial part of the n th mode solution to the field equations, i.e. the n th mode function. We consider the field and the detector as being all in a stationary cavity in flat space time. The cavity introduced here for the vacuum field and the associated infrared and ultraviolet mode cutoff. In order to determine these mode functions, we need to impose boundary conditions for the cavity. The different boundary conditions are with different advantages. For example,

$$\begin{aligned} u_n(x, t) &= \frac{1}{\sqrt{k_n L}} \exp(-i\omega_n t) \sin[k_n x] \text{ or} \\ u_n(x, t) &= \frac{1}{\sqrt{k_n L}} \exp(-i\omega_n t) \exp[k_n x] \end{aligned} \quad (8)$$

the above is from the reflecting boundary condition or periodic boundary condition respectively. Here k_n is the wave vector for the n th field mode. For the massless scalar field, $\omega_n = |k_n|$ and $k_n = n\pi/L$ is under the reflecting boundary conditions or $k_n = 2n\pi/L$ is under the periodic boundary conditions where L is the length of the cavity. The periodic boundary condition is preferred in our study because it can avoid the blue-shift induced decoupling. [23] The monopole moment of the detector $\hat{\mu}$ in the Schrödinger picture gives as

$$\hat{\mu}^S = \hat{a}_d + \hat{a}_d^\dagger \quad (9)$$

where \hat{a}_d and \hat{a}_d^\dagger are the annihilation and creation operator respectively for the detector. Now, we write down

the whole Hamiltonian \hat{H}^S in the Schrödinger picture with respect to the detector's proper time under the transformation table as

$$\begin{aligned}\hat{H}^S &= \hat{H}_0^S + \hat{H}_1^S \\ &= \frac{dt(\tau)}{d\tau} \sum_n \omega_n \hat{a}_n^\dagger \hat{a}_n + \Omega \hat{a}_d^\dagger \hat{a}_d \\ &\quad + \lambda(\tau) (\hat{a}_d + \hat{a}_d^\dagger) \sum_n (\hat{a}_n v_n[x(\tau)] + \hat{a}_n^\dagger v_n[x(\tau)])\end{aligned}\quad (10)$$

where Ω is the characteristic frequency of the detector. The first terms of the above equation represent the Hamiltonian of the scalar field. The second term represents the Hamiltonian of the detector. The third terms represent the interactions between the field (modes) and the detector. Notice that the form of the complete Hamiltonian in the Heisenberg picture coincides with the form of the Hamiltonian in the Schrödinger picture. It is straightforward to write the most general $X - X$ type Hamiltonian for an arbitrary number of detectors moving on general trajectories with different proper times τ_j and with the time dependent couplings.

$$\begin{aligned}\hat{H}^H &= \hat{H}_0^H + \hat{H}_1^H \\ &= \sum_{n=1}^N \omega_n \hat{a}_n^\dagger \hat{a}_n + \sum_{j=1}^M \frac{d\tau_j}{dt} [\Omega \hat{a}_{d_j}^\dagger \hat{a}_{d_j} \\ &\quad + \sum_{n=1}^N \lambda_{nj}(t) (\hat{a}_{d_j} + \hat{a}_{d_j}^\dagger) (\hat{a}_n v_n[x(\tau)] + \hat{a}_n^\dagger v_n[x(\tau)])]\end{aligned}\quad (11)$$

Here the first terms of the above equation represents the Hamiltonian of the scalar field. The second terms represent the Hamiltonian of the detectors. The third terms represent the interactions between the field (modes) and the detectors. From Eq.(11), a natural IR cutoff of the field modes is introduced due to our cavity setting with a length L . A UV cutoff is introduced for the sake of the computation and the resolution of the detectors.

C. Evolution dynamics of the detectors

Conventionally, two main approaches to quantum information processing have been pursued. [25] On the one hand, quantum information is encoded into the systems with a discrete, finite number of degrees of freedom such as qubits. Typical examples of qubit implementations are the nuclear spins of individual atoms in a molecule, the polarization of the photons, the ground/excited states of trapped ions, etc. On the other hand, a continuous approach has also been investigated. This is based on the quantum information and the correlations encoded in the degrees of freedom through the continuous variables.

Typical examples of the continuous variable implementations are the position and momentum of a particle etc. In this study, we will mainly use the second approach. Specifically, both the detectors and the scalar field modes are described as continuous-variables to account the underlying bosonic degrees of freedom. We will use the Hamiltonian Eq.(11) in the Heisenberg picture to evolve the quadrature operators ($\hat{q}_{d_j}(t), \hat{p}_{d_j}(t)$) for each detector and ($\hat{q}_n(t), \hat{p}_n(t)$) for each field mode, where j runs over all detectors and n for all field modes. These coordinate and momentum operators satisfy the standard canonical commutation relations as follows: $[\hat{q}_{d_j}(t), \hat{p}_{d_j}(t)] = i\delta_{ij}$, $[\hat{q}_n(t), \hat{p}_k(t)] = i\delta_{nk}$. We organize these operators in a phase-space vector form as

$$\hat{X} = (\hat{q}_{d_1}, \hat{p}_{d_1}, \dots, \hat{q}_{d_j}, \hat{p}_{d_j}, \dots, \hat{q}_1, \hat{p}_1, \dots, \hat{q}_n, \hat{p}_n) \quad (12)$$

The vector \hat{X} in a phase-space naturally has a symplectic form $[\hat{X}, \hat{X}^T] = i\Delta = i \oplus_i \begin{bmatrix} 0 & 1 \\ -1 & 0 \end{bmatrix}$, where i runs through all the degrees of freedom (both detectors and field modes). We will consider the state of our detector-field system to be a Gaussian states, [26] for a continuous variable ensemble. A Gaussian state is defined as any state whose characteristic functions and quasi-probability distributions are Gaussian functions in the quantum phase space. In general, a Gaussian state is fully characterized by its first and second canonical moments only. [25] In our study, a Hamiltonian that is quadratic in the operators with no linear terms as Eq.(11) is considered. As a result, all states are Gaussian with no-displacement, and all evolutions are homogeneous Gaussian unitary. Therefore, we may neglect the first moments and the state is fully described by the second moments or the covariance matrix σ .

$$\sigma_{ij} = \langle \hat{x}_i \hat{x}_j + \hat{x}_j \hat{x}_i \rangle - 2 \langle \hat{x}_i \rangle \langle \hat{x}_j \rangle \quad (13)$$

The time evolution of the entire covariance matrix, including both the detector and the field, is governed by the equation of unitary evolution

$$\sigma(t) = S(t)\sigma(0)S^T(t) \quad (14)$$

Here, S is a symplectic matrix: $S\Delta S^T = \Delta$ and $\hat{X}(t) = S(t)\hat{X}(0)$. In Hilbert space, the evolution of a state is dependent on the time evolution operator \hat{U} , S plays the same role in the quantum phase space. A general time-dependent, quadratic, Heisenberg-picture Hamiltonian can be written as

$$\hat{H} = \hat{X}^T F(t) \hat{X} \quad (15)$$

Here $F(t)$ is a Hermitian matrix of the c-numbers only determined by the explicit time-dependence of the Hamiltonian. For more details about deriving $F(t)$, please see

Appendix A. The Heisenberg equation for the time evolution of the quadratures is given by

$$\frac{d\hat{X}}{dt} = i[\hat{H}, \hat{X}] \quad (16)$$

Using Eq.(15) Eq.(16) and the definition of Δ , one derives

$$\frac{d\hat{X}}{dt} = \Delta F^{sys} \hat{X} \quad (17)$$

Here $F^{sys} = F + F^T$. This is just the quantum phase space version of the Schrödinger equation. Using $\hat{X}(t) = S(t)\hat{X}(0)$ and $[\hat{X}, \hat{X}^T] = i\Delta$, finally we get

$$\frac{d\hat{S}}{dt} = \Delta F^{sys} S(t) \quad (18)$$

Note that once we solve Eq.(18) with the initial condition $S(0) = I$ such that $\hat{X}(0) = S(0)\hat{X}(0)$, we know the evolution of the detectors-field system. In the particular simple cases where the Hamiltonian at different times commute, the solution of Eq.(18) can be obtained analytically and it is simply $S(t) = \exp[\Delta F^{sys}t]$. From Eq.(11), a natural IR cutoff of field modes is introduced due to our cavity setting with a length L . A UV cutoff is introduced for the sake of the computation and the resolution of the detectors. We provide an effective criterion to choose a reasonable cutoff with required arbitrary high precision depending on causality analysis in Appendix B.

III. RESULT

A. Quantum correlation measures: entanglement, mutual information and discord

1. Covariance and S matrix evolution

In what follows, we will consider two accelerated detectors which are moving inside a stationary cavity in flat space-time. The two separable detectors are initially stationary inside the cavity. The detectors are made as harmonic oscillator rather than a qubit. They both have the same characteristic frequency Ω . We focus on the one dimensional dynamics, so we choose a smooth cavity with length L . Therefore, there is a natural *IR* cutoff for the field modes A *UV* cutoff is introduced for the sake of the computation and the resolution of detectors. The Hamiltonian reads

$$\begin{aligned} \hat{H}^{accelerated} = & \sum_{n=1}^N \omega_n \hat{a}_n^\dagger \hat{a}_n + \sum_{j=1}^2 \frac{d\tau_j}{dt} [\Omega \hat{a}_{d_j}^\dagger \hat{a}_{d_j} \\ & + \sum_{n=1}^N \lambda_{nj}(t) (\hat{a}_{d_j} + \hat{a}_{d_j}^\dagger) (\hat{a}_n v_n[x(\tau)] + \hat{a}_n^\dagger v_n[x(\tau)])] \end{aligned} \quad (19)$$

$$\begin{aligned} \hat{H}^{stationary} = & \sum_{n=1}^N \omega_n \hat{a}_n^\dagger \hat{a}_n + \sum_{j=1}^2 [\Omega \hat{a}_{d_j}^\dagger \hat{a}_{d_j} \\ & + \sum_{n=1}^N \lambda_{nj}(t) (\hat{a}_{d_j} + \hat{a}_{d_j}^\dagger) (\hat{a}_n v_n[x(\tau)] + \hat{a}_n^\dagger v_n[x(\tau)])] \end{aligned} \quad (20)$$

From the above Hamiltonian, F^{sys} can be derived. From Eq.(18): $\frac{dS}{dt} = \Delta F^{sys} S(t)$, we can calculate the evolution of the symplectic matrix $S(t)$.

An accelerated detector will experience a thermal bath in which the temperature is associated with $T = a/2\pi$, where a is the proper acceleration of the detector. The initial continuous variables for the covariances read

$$\sigma_f^0 = I_{2N} \quad (21)$$

or

$$\sigma_f^0 = \oplus_i \begin{bmatrix} v_i & 0 \\ 0 & v_i \end{bmatrix} \quad (22)$$

Eq.(21) denotes a field at vacuum state (I_{2N} is an identity matrix) and Eq.(22) denotes a field at thermal state, where $v_i = \frac{\exp(\frac{\omega_i}{T})+1}{\exp(\frac{\omega_i}{T})-1}$, and T is the temperature of the field. [25]

$$\sigma_d^0 = I_4 \quad (23)$$

Eq.(23) is for both accelerated and stationary detectors. The initial continuous covariance matrix of the whole system is given as

$$\sigma(0) = \sigma_d^0 \oplus \sigma_f^0 \quad (24)$$

Once determined from the Eq.(14) $\sigma(t) = S(t)\sigma(0)S^T(t)$, the covariance matrix evolution of our system can be obtained and will take the generic form

$$\sigma(t) = \begin{bmatrix} \sigma_d & \gamma \\ \gamma^T & \sigma_f \end{bmatrix} \quad (25)$$

Here σ_d and σ_f represent the $4M \times 4M$ and $4N \times 4N$ covariance matrices of the reduced states of the M detectors and N field modes, respectively. The matrix γ contains the information regarding the correlations between the detectors and the field. We can compute the correlation measures between the detectors such as the logarithmic negativity for entanglement, the mutual information, and quantum discord. The covariance matrix of the detector-detector state that we obtain upon evolution will be in the generic form (only considering the two detectors case here)

$$\sigma(t) = \begin{bmatrix} \sigma_{d_1} & \gamma_{12} \\ \gamma_{12}^T & \sigma_{d_2} \end{bmatrix} \quad (26)$$

As in Eq.(26), σ_{d_1} and σ_{d_2} describe the reduced states of detectors 1 and 2 respectively. The matrix γ_{12} stores information regarding the correlations between the two detectors. As an example, the detectors will be uncorrelated (i.e., in a product state) if and only if all entries of γ_{12} are zero.

2. Quantum Correlations: entropy, entanglement, mutual information and discord

The Von Neumann entropy of a general Gaussian state can be given by [24]

$$S_{VN}(\sigma) = \sum_{i=1}^N s(v_i) \quad (27)$$

$$s(x) = \frac{x+1}{2} \log_2\left(\frac{x+1}{2}\right) - \frac{x-1}{2} \log_2\left(\frac{x-1}{2}\right) \quad (28)$$

Here v_i is the i th symplectic eigenvalue.(i.e. the orthogonal eigenvalues of the matrix $|i\Delta\sigma|$) The mutual information between the detectors, which quantifies the total amount of the correlation between the subsystems that can potentially be useful for the computational tasks, then follows the usual form [6],

$$I_{MI} = S_{VN}(\sigma_{d_1}) + S_{VN}(\sigma_{d_2}) - S_{VN}(\sigma_d) \quad (29)$$

It is easy to see when $\gamma_{12} = 0$, $I = 0$, then there is no correlation between the two detectors. Defining the quantities $\alpha = \text{Det}[\sigma_{d_1}]$, $\beta = \text{Det}[\sigma_{d_2}]$, $\gamma = \text{Det}[\gamma_{12}]$ and $\delta = \text{Det}[\sigma_d]$, then the logarithmic negativity for characterizing the entanglement between the detectors is given as [24]

$$E_N = \text{Max}[0, -\log_2(\tilde{v}_-)] \quad (30)$$

where \tilde{v}_- is the smaller of the state's partially transposed symplectic eigenvalues which is given by $\tilde{v}_- = \sqrt{\frac{\tilde{\Delta} - \sqrt{\tilde{\Delta}^2 - 4\delta}}{2}}$, where $\tilde{\Delta} = \alpha + \beta - 2\gamma$.

The quantum discord is a measure of the pure quantum part of the correlations obtained by subtracting off the classical correlations from the mutual information. It is a measure of the information that cannot be extracted without the joint measurements. The discord is a good indicator of the quantum nature of quantum correlation. [5]It is given by [27]

$$D(1:2) = s(\sqrt{\beta}) - s(\sqrt{v_1}) - s(\sqrt{v_2}) + s(\sqrt{E}) \quad (31)$$

where v_1 and v_2 are the symplectic eigenvalues of σ_d and E is defined as

$$E = \begin{cases} = \frac{2\gamma^2 + (-1 + \beta)(-\alpha + \beta)}{(-1 + \beta)^2} \\ + \frac{2|\gamma|\sqrt{\gamma^2 + (-1 + \beta)(-\alpha + \beta)}}{(-1 + \beta)^2} \\ \text{for } (-\alpha\beta + \delta)^2 \leq (-1 + \beta)(\alpha + \delta)\gamma^2 \\ = \frac{\alpha\beta - \gamma^2 + \delta}{2\beta} \\ - \frac{\sqrt{\gamma^4 + (-\alpha\beta + \delta)^2 - 2\gamma^2(\alpha\beta + \delta)}}{2\beta} \\ \text{otherwise} \end{cases} \quad (32)$$

In general, the discord is not symmetric $D(1:2) \neq D(2:1)$.

B. Equilibrium Quantum Correlations Between the Two Equally Accelerated Detectors

1. Accelerations of the Detectors in the Same Direction

1) Entanglement

In what follows, we will consider the two detectors which are in the equilibrium state. This means that they are either stationary and have the same temperature or have the same accelerated motion in the cavity. The world line can be given by $(t, \pi, 0, 0)$ and $(t, 2\pi, 0, 0)$ for the two stationary detectors named as Alex and Robb while $(a^{-1} \sinh(a\tau), a^{-1}(\cosh(a\tau) - 1), 0, 0)$ and $(a^{-1} \sinh(a\tau), a^{-1}(\cosh(a\tau) - 1 + a\pi), 0, 0)$ for the two accelerated detectors Alice and Bob respectively. We have several setups for the considerations: a) two detectors accelerate with the same acceleration while they start from the vacuum state; b) two separated detectors start at vacuum state initially and then stationarily immersed in a thermal field. We are interested in exploring the behaviors of the entanglement and the mutual information as well as the quantum discord between detectors from the field in different settings. In a cavity, the effect of the boundary on the detector's interaction with the quantum field becomes important especially for an accelerated detector. The authors dodged the boundary effect by arranging a series of cavities wall to wall in [28] In this study, we adopt another approach which considers the interaction between the detectors and the field is switch on far away from the edge (as was considered in [29] to avoid the boundary effect. To do so, we consider the Gaussian distribution in time, i.e. $\lambda(\tau) = \lambda_0 \exp(-\frac{(\tau - \tau_0)^2}{2\varepsilon})$. Through this setting the accelerated detector decouples to the field when the detector is close to the boundary.

The logarithmic negativity E_N between the detectors is a measure of the entanglement. We show this entanglement measure in two cases in Figure 1(a) 1(b), Figure

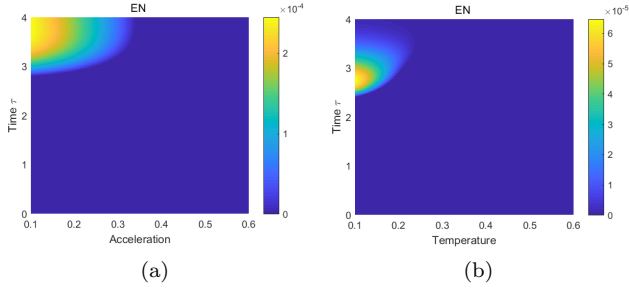


FIG. 1. Figure 1(a) describes how E_N varies with respect to the acceleration and the proper time τ . One starts from a lower acceleration 0.1, while the two detectors accelerate with the same proper acceleration and always stay at a distance π from each other. Figure 1(b) describes how E_N varies with respect to the temperature of the field and proper time τ . One starts from a lower temperature 0.1, while the two detectors are stationary at a distance π from each other. The acceleration corresponds to the temperature from Unruh effect $T = \frac{a}{2\pi}$. The cavity length is 4π , while the detector's response frequency is set as $\Omega = 3/2$, which indicates that the detector is in resonance with the 3th field mode. That means we can just consider finite modes as the higher energy modes are hard to response to the detector. The number of field modes is set as 40, and the coupling strength for both detectors is set as $\lambda(\tau) = 0.05 \exp(-\frac{(\tau-1.5)^2}{2})$.

1(a) depicts E_N between the two accelerated detectors varying with the acceleration and the proper time. Figure 1(b) depicts E_N between the two stationary detectors varying with respect to the temperature of the field and the proper time (equals to the coordinate time). The reason we choose the proper time is clear: the period of the correlation dynamics of the accelerated detectors associated with the response frequency of the detector is a constant in the detector's proper time. In other words, we can avoid the redshift effect that appears in the coordinate time.

Due to the cavity setting, the plot range is limited. Strictly speaking, we can only see part of the effect of the detectors, especially for the accelerated detectors. Nevertheless, we have still found some interesting behaviors. Firstly, the two detectors initially unrelated can harvest the entanglement from the field. The accelerated detectors harvest later than the stationary detectors. Although the quantitative details are different between the two cases, the overall qualitative trend in time and in acceleration (temperature) is similar. Entanglement resurrects from the death and dies again in time. This behavior appears later in time for the accelerated detectors than that for the stationary detectors in the thermal bath.

The possible explanation for the fluctuating oscillation pattern in time of the entanglement might be the quantum recurrence (live and die) behavior from the non-Markovian effect [30]. The non-Markovian effect can lead to the information back flow from the system to the en-

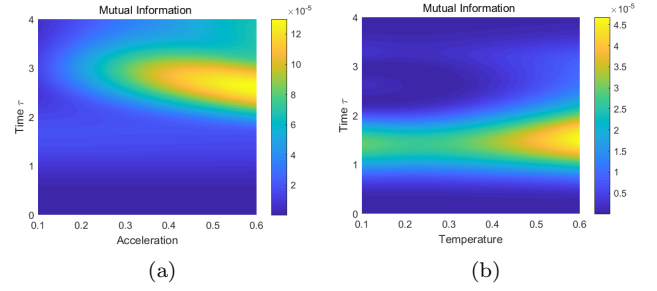


FIG. 2. Figure 2(a) describes how mutual information varies with respect to the acceleration and proper time. One starts from a lower acceleration 0.1, while the two detectors accelerate with the same proper acceleration and are at a distance π from each other. Figure 2(b) describes how the mutual information varies with respect to the temperature of field and the time. One starts from a lower temperature 0.1, while the two detectors are stationary at a distance π from each other. All parameters are the same as those in Figure 1(a) 1(b).

vironment. [31] The eventual decreasing trend of the entanglement in time may come from the fact that at long times the systems reach equilibrium being lack of the quantum nature of the thermal mixed states. Besides, the coupling constant decreases over time once $\tau > \tau_0$. We can then omit the memory effect of the environment, considering that there is no feedback from environment to system as long as the coupling to the environment is weak enough. [32]

At fixed times, as the acceleration (temperature) increases, the entanglement decreases monotonically. This is from the Unruh effect: the local acceleration is equivalent to the temperature. When the acceleration or equivalently the temperature is high enough, there is no entanglement in Figure 1(a) 1(b). As the acceleration (temperature) increases, the thermal effects become more pronounced and the decoherence becomes more significant, leading to reduced entanglement. Noticed that the entanglement reduction is relatively faster for the stationary detectors in a thermal bath than that for the accelerated detectors.

2) Quantum Mutual Information and Quantum Discord

The mutual information between the two detectors, which quantifies the total quantum correlation, is shown in Figure 2(a) 2(b). In our setting, the quantum mutual information has almost the same trend in time and acceleration (temperature) compared to the quantum discord. For the sake of simplicity, we just consider the quantum discord in details. The statement also holds for the mutual information.

We plot in Figure. 3(a) 3(b) the quantum discord between the detectors in the same scenario as Figure. 3(a) 3(b). Quantum discord is a measure of the pure quantum part of the correlations obtained by subtracting off the classical correlations from the quantum mutual information. The trend in Figure 3(a) 3(b) for the

quantum discord are very similar to that for the quantum mutual information in Figure 2(a) 2(b). The quantum discord (mutual information) varies with the acceleration and time or the temperature and time. Their behaviors in time are quite similar to that of the entanglement E_N . This can follow the same explanation on the entanglement of E_N with the quantum recurrence. Again we see that the quantum recurrence appears later in time for the accelerated detectors than that for the stationary detectors in the thermal bath. The difference is that the quantum discord (mutual information) is amplified by the higher temperature rather than being reduced as in the case of entanglement.

At higher acceleration or temperatures, the quantum discord (mutual information) is more robust than the entanglement E_N . Moreover, as the acceleration (temperature) of the stationary detectors increases, the quantum discord can be amplified via increasing the temperature consistent with the results in Ref [24]. The entanglement and quantum discord has a monogamic relationship in a tripartite system (two subsystems in an environment) [33]. Moreover, Ref [34] shows that the evolution of the discord reflects the entanglement entropy dynamics between the system and the environment, and its behavior is opposite to the entanglement between the (sub)systems. This implies that increasing the temperature of the field can lead the detectors to be more mixed and therefore more likely to be entangled with the environment in our case. This leads to an increased amount of discord (mutual information) but less entanglement between the detectors. Also noticed that the discord (mutual information) enhancement is relatively faster for the accelerated detectors than that for the stationary detectors in a thermal bath.

Unlike the entanglement E_N , the quantum discord (mutual information) may exist for long and still fluctuate over time in Figure 2(b). We suggest that the evolution of the quantum discord (mutual information) in such systems can be understood as a competition between the decoherence effect among the systems due to the environment (field) and the system-environment (detectors-field) entanglement that such decoherence also tends to generate. As we have seen, in this case the latter wins. The quantum discord is sustained due to the dominant system-environment (detector-field) entanglement over the decoherence or the disentanglement from the system (detector-detector). On the other hand, the system-environment entanglement does not boost the entanglement within or between the systems. Indeed, due to monogamy, the entanglement is usually further damaged and therefore easier to be destroyed as shown in Figure 1(b).

There are also apparently differences between the effects of the temperature of the flat space and the effects of the corresponding accelerations. Meanwhile, in [35], it was shown that the entanglement profiles of the two accelerated qubit detectors and the two stationary qubit detectors in the thermal field are largely the same but

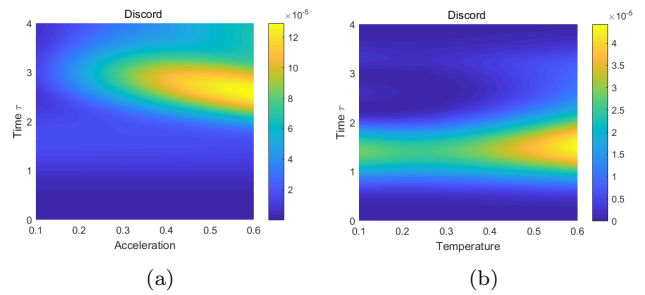


FIG. 3. Figure 3(a) describes how quantum discord varies with respect to the acceleration and the proper time. One starts from a lower acceleration 0.1, while the two detectors accelerate with the same proper acceleration and are at a distance π from each other. Figure 3(b) describes how quantum discord varies with respect to the temperature and the proper time. One starts from a lower temperature 0.1, while the two detectors are stationary at a distance π from each other. All parameters are the same as those in Figure 1(a) 1(b).

with certain differences. The correlation function plays an important role in quantifying the entanglement. Although a single accelerated detector is equivalent to a stationary detector in the thermal bath, this does not guarantee the equivalency of the quantitative correlation between the two accelerated detectors and the correlation between the two stationary detectors in the thermal bath, since intuitively the detectors of the latter are surrounded by a global thermal bath while the detectors of the former are located locally surrounded by the associated local thermal baths. [35] [36] Here we can see the similarities and the differences between the effects of the temperature of the flat space and effects of the corresponding accelerations or equivalently local curvature on the entanglement, quantum mutual information and quantum discord. We can see that although the Unruh and Hawking pointed out the equivalence of the temperature and the acceleration, they are locally equivalent. The temperature and the acceleration show certain different impacts on the global correlations such as entanglement, mutual information and discord. For a detector in a sealed elevator, it is difficult for him to identify whether it is stationary in a thermal field or accelerating. However, it is possible for the two detectors to differentiate that through examining their global correlation. For example, the stationary detectors in the thermal field can have the access to the quantum correlation faster than that of the accelerated detectors.

2. Accelerations of the Detectors in the Opposite Directions

We now investigate the entanglement, the quantum mutual information and the quantum discord between the two accelerated detectors in the opposing direction. The world lines are $(a^{-1} \sinh(a\tau), (a^{-1} \cosh(a\tau) - 1 + 2a\pi), 0, 0)$ and $(a^{-1} \sinh(a\tau), -a^{-1}(\cosh(a\tau) - 1 -$

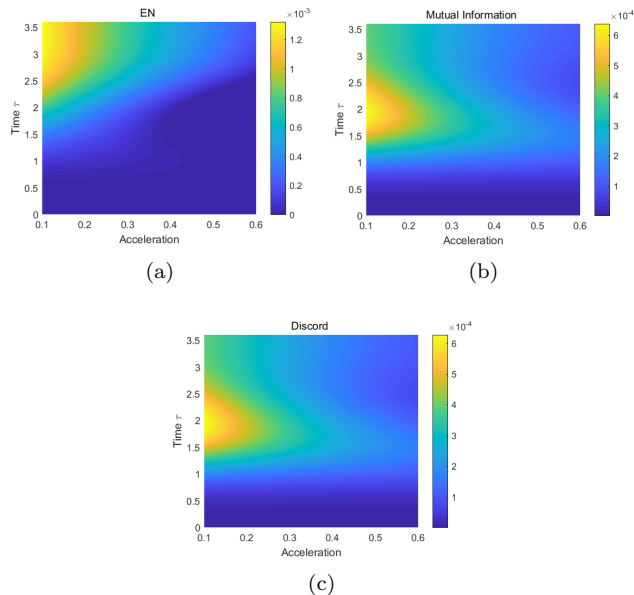


FIG. 4. Figure 4(a) 4(b) 4(c) describes how entanglement E_N , quantum mutual information and quantum discord varies with respect to the acceleration and proper time τ . One starts from a lower acceleration 0.1 and the two detectors accelerate with the same proper acceleration in two opposing directions starting at 2π . The coupling strength for both detectors is set as $\lambda(\tau) = 0.05 \exp(-(\tau - 1.5)^2)$. All parameters are the same as those in Figure 1(a) 1(b).

$2a\pi, 0, 0$) for Alice and Bob respectively. This mimics the two heat sources in flat space time moving away from each other. From Figure 4(a) 4(b) 4(c), as the time goes by, the two detectors are further away from each other at a constant acceleration; this is also true over acceleration at fixed time. They all resurrect from death over time. And the quantum correlation decreases monotonically over the acceleration at fix time. Once again, we see the Unruh effect of bipartition. The higher acceleration (temperature) leads the detectors to be more classical being lack of quantum nature. This results to the decrease in the entanglement. Since the larger acceleration means more distant detectors at fixed time, the mutual information (discord) is not amplified by the higher acceleration but reduced. This shows that the distance effect dominates the evolution. We suggest that the evolution of the quantum discord (mutual information) in such systems can be understood as a competition between the distance effect among the detectors due to the opposite acceleration and the thermal amplification that such acceleration tends to generate. As we have seen, in this case the former wins.

C. Nonequilibrium Quantum Correlations Between the Two Different Accelerated Detectors

1. Nonequilibrium Quantum Correlations Between the Equally Accelerated Detectors from the Coupling Differences to the Scalar Field

1) Quantum Entanglement

In this part, we will consider a nonequilibrium case with the coupling strengths between each detector and the scalar field in the cavity being different from each other. The nonequilibriumness is characterized by the degree of the detailed balance breaking due to the different couplings of the detectors to the vacuum field. One can understand it this way, if the two detectors are with the different accelerations, then according to the Unruh effects, the two detectors are surrounded by the environments with the different temperatures. The temperature difference creates the nonequilibrium condition. On the other hand, if the couplings of the accelerated detectors to the scalar field are different, then the occupation or the number density for the detectors would be different for the two detectors since they are not only dependent on the local temperatures but also on the couplings to the scalar field. This also creates an imbalance or nonequilibrium condition. Moreover, the non-Markovian dynamics depending on the coupling constant can lead to the information back flow from the system to the environment as we mentioned above. Differences in the coupling constants of the two detectors can give rise to the nonequilibriumness and the associated behaviors.

We first consider the quantum correlations in the different coupling strengths with the equal accelerations since we would like to separate the pure effects of the nonequilibriumness from that of the increased distance due to the accelerations. The world line is given as $(t, \pi, 0, 0)$ and $(t, 2\pi, 0, 0)$ for the two stationary detectors Alex and Robb respectively, while $(a^{-1} \sinh(a\tau), a^{-1}(\cosh(a\tau) - 1), 0, 0)$ and $(a^{-1} \sinh(a\tau), a^{-1}(\cosh(a\tau) - 1 + \pi), 0, 0)$ are for the two accelerated detectors Alice and Bob respectively. The coupling is assumed to be a constant over time and we set $\lambda_1 + \lambda_2 = \text{Constant}$. The entanglement is recurrent and dies again over time similar to the equilibrium case. At fixed proper times, we can see that non-trivial nonequilibrium effect which can amplify the entanglement for the accelerated case in Figure 5(a) but tend to decrease the entanglement for the stationary case under the thermal bath in Figure 5(b). This nontrivial dependence of the entanglement versus the nonequilibriumness maybe from the competition of the coherence and population redistribution. [37]

2) Quantum Mutual Information and Quantum Discord

We depict the quantum mutual information and discord with respect to the coupling difference and time at the same temperature and the same acceleration in Figure 6(a) 6(b). In our setting, we find that the quan-

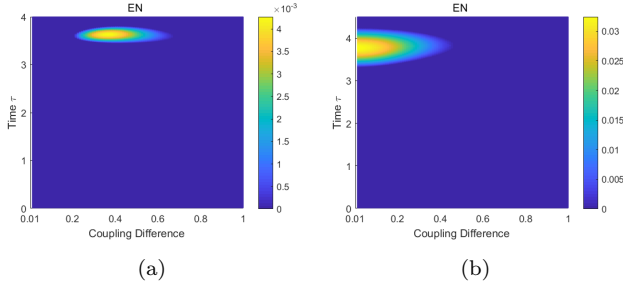


FIG. 5. Figure 5(a) describes how E_N varies with respect to the coupling difference and proper time. Alice and Bob stay at a lower constant proper acceleration 0.2, and at a distance π apart. Figure 5(b) describes how E_N varies with respect to the coupling difference and time. Alex and Robb are stationary at thermal equilibrium at lower temperature 0.1 and also stay a distance π apart. All parameters are the same as those in Figure 1(a) 1(b) except λ is a constant over time.

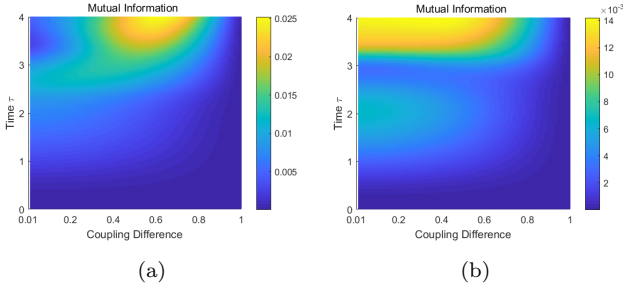


FIG. 6. Figure 6(a) describes how quantum mutual information varies with respect to the coupling difference and the proper time. Alice and Bob stay at a lower constant proper acceleration 0.2, and at a distance π apart. Figure 6(b) describes how mutual information varies with respect to the coupling difference and time. Alex and Robb are stationary at thermal equilibrium at lower temperature 0.1 and also stay a distance π apart. All parameters are the same as those in Figure 1(a) 1(b).

tum mutual information has almost the same trend compared to the quantum discord. For the sake of simplicity, we will only discuss the quantum discord in details, the statement also holds for the quantum mutual information.

The quantum mutual information and quantum discord behave non-monotonously in time and show the recurrent behavior. At fixed proper time, the quantum mutual information and quantum discord can be enhanced by the coupling difference which characterizes the nonequilibrium through the degree of the detailed balance breaking in a large coupling difference range. Eventually, the quantum mutual information and quantum discord can be reduced as the coupling difference becomes large. These behaviors lead to a wide coupling difference zone for the detectors to harvest the quantum

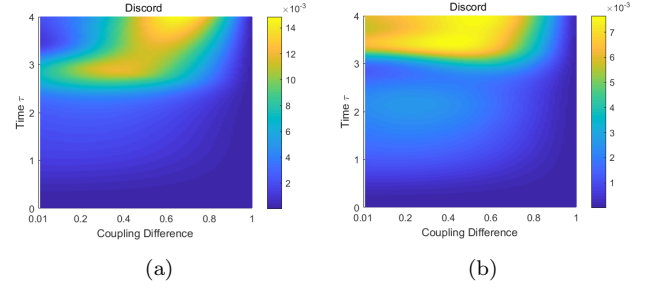


FIG. 7. Figure 7(a) describes how quantum discord varies with respect to the coupling difference and the proper time while Alice and Bob stay at a lower constant proper acceleration 0.2, and at a distance π apart. Figure 7(b) describes how quantum discord varies with respect to the coupling difference and time while Alex and Robb are stationary at thermal equilibrium at lower temperature 0.1 and also stay a distance π apart. All parameters are the same as those in Figure 1(a) 1(b).

correlation from the nonequilibrium scenario. The similar behaviors were also observed in Ref [37] for the quantum correlations between the two qubits (stationary detectors) in the nonequilibrium environments as the result of the competition between the coherence and the population. At fixed proper time, we also observe that the mutual information (discord) from the accelerated detectors is enhanced faster and becomes larger than that from the stationary detectors in a thermal bath. This seems to imply that accelerated nonequilibriumness is more efficient for enhancing the mutual information (discord) than the stationary counterpart.

The enhancement of the quantum correlations is apparent from the higher coupling difference or the nonequilibriumness under the higher local accelerations (or equivalently effective local space time curvature). Here we give a rationale for the enhancement of the quantum correlations through the nonequilibriumness. The nonequilibriumness creates the net energy flow to the system much like a voltage can generate the electric current. Since the flow is global in state space, the enhanced flow from the nonequilibriumness can therefore increase the global correlations.

2. Nonequilibrium Quantum Correlations Between the Detectors with Different Accelerations

In this part, we will consider the case where the two detectors in the cavity are in nonequilibrium state with different accelerations or equivalently different local space time curvatures. The world line is $(a^{-1} \sinh(a\tau), a^1(\cosh(a\tau) - 1), 0, 0)$ and $(b^{-1} \sinh(b\tau), b^1(\cosh(b\tau) - 1), 0, 0)$ for the two detectors Alice and Bob respectively.

Since there are different proper times associated with the accelerations, we chose a viewpoint from the larger

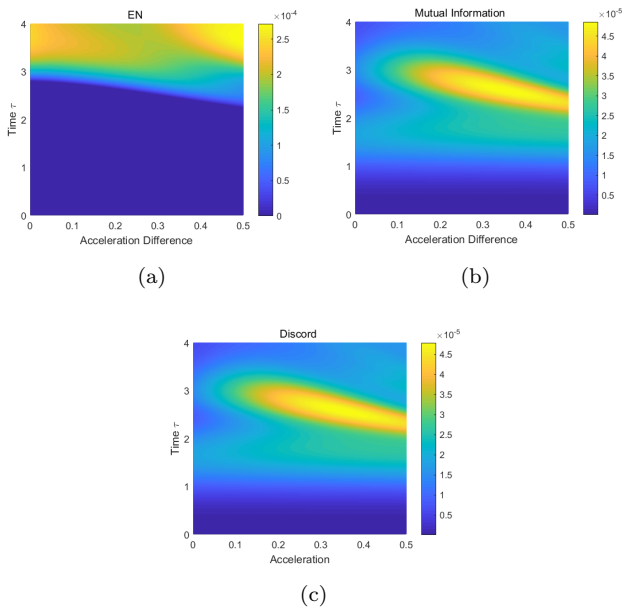


FIG. 8. Figure 8(a) 8(b) 8(c) describes how E_N , mutual information and quantum discord vary with respect to the acceleration difference and the Bob's proper time τ . Alice stays at a lower acceleration 0.1 and Bob has a larger acceleration starting from 0.1. All the parameters are the same as those in Figure 1(a) 1(b).

acceleration detector to weaken the redshift effect. Meanwhile, we provide the plots which show the significant redshift effect in the coordinate time in the Appendix C. The quantum correlations resurrect over time. The quantum correlations can be amplified over the acceleration difference. The acceleration difference can be viewed as the nonequilibriumness measure (temperature difference through Unruh effect). The acceleration difference can also lead to the change in distance between the two detectors. Therefore, there are two effects of the two detectors: the larger distance and bigger difference in accelerations which both influence the quantum correlation. The nonequilibriumness can amplify the quantum correlations while the larger distance can weaken the quantum correlations. One can see the amplification of the quantum correlations as a result of the competition between the nonequilibriumness and the distance. We see that the nonequilibrium effects dominate the distance effects on the quantum correlations.

IV. CONCLUSION

Using the developed methods, we discuss the difference of the equilibrium quantum correlations such as entanglement, mutual information and quantum discord between the two equally accelerated detectors and that between the two stationary detectors in thermal field with temperature T . Firstly, there is quantum correlation har-

vesting from the field over time in different scenarios. The information back flow from the system to the environment may be caused by the non-Markovian effect. The acceleration and the temperature have qualitatively similar trends on the quantum correlation of bipartition. This shows the similar effects from the two equally detectors under the equal acceleration and the same temperature. As the acceleration (temperature) or equivalently local curvature of the stationary detectors increases, the entanglement disappears, while the mutual information and the quantum discord is enlarged. The reason for this is given: the quantum discord (mutual information) is sustained due to the dominant system-environment (detector-field) entanglement over the decoherence or the disentanglement from the system (detector-detector). On the other hand, the system-environment entanglement does not boost the entanglement within or between the systems. Indeed, due to monogamy, the entanglement is usually further damaged. We also observe that the recurrence of the quantum correlations appear later in time for the accelerated detectors than that for thermal stationary detectors. At fixed time, the entanglement reduction is relatively faster for the stationary detectors in a thermal bath than that for the accelerated detectors, while the discord (mutual information) enhancement is relatively faster for the accelerated detectors than that for the stationary detectors in a thermal bath. The quantum correlation between the detectors accelerated in the opposite direction has also been studied. Remarkably, the quantum correlations decrease monotonically over the acceleration. We suggest that the evolution of quantum discord (mutual information) in such systems can be understood as a competition between the distance effect among the detectors due to the opposite acceleration and the thermal amplification that such acceleration also tends to generate. As we have seen, in this case the former wins.

In the meanwhile, we also study the nonequilibrium quantum correlations. We first consider the nonequilibrium effect caused by the different couplings. We pointed out that the nonequilibriumness characterized by the degree of the detailed balance breaking caused by different couplings can strengthen the quantum correlations. This leads to a wide range of the coupling difference zone to harvest the quantum correlations for nonequilibrium scenarios. At fixed proper time, we also observe that the mutual information (discord) from the accelerated detectors is enhanced faster and becomes larger than that from the stationary thermal detectors. This suggests that accelerated nonequilibriumness may be more efficient for enhancing the mutual information (discord) than the stationary counterpart. Another nonequilibrium case we consider is that the two accelerated detectors with different accelerations or equivalently different local space time curvatures. This generates both the nonequilibrium effect and the distance effect on the quantum correlations between the two detectors. The nonequilibrium effect appears to dominate the distance effects in terms of enhancing the quantum correlations.

To give a rational for the nonequilibrium enhanced quantum correlations, we note that the nonequilibriumness creates the net energy flow to the system much like the voltage generates the electric current. Since the flow is global in state space, the enhanced flow can increase the global correlations.

On the other hand, since the mass and energy is equivalent under the Einstein mass-energy relationship, the increase of the nonequilibriumness leads to the increase of the energy flow and therefore the contrasts in the effective mass of the system. Since the local curvature of the space-time geometry is dependent on the mass of the system, the increase of the nonequilibriumness can enhance the contrasts in the local effective space-time curvature. An increased contrast in local curvature can create contrasts in local space time fluctuations. This can decrease the effective distance for the communications. Thus one expects the nonequilibriumness can enhance the quantum correlations through the global energy flow or effectively reducing the distances between the objects.

ACKNOWLEDGMENTS

He Wang acknowledges support of National Natural Science Foundation of China Grants 21721003, Ministry of Science and Technology of China Grants 2016YFA0203200.

Appendix A: Derivation of $F(t)$

For a general time-dependent, quadratic Hamiltonian, it's convenient to express in the form of annihilation (creation) operator vector, which is defined as follows

$$\hat{a} = [\hat{a}_{d_1}, \hat{a}_{d_2}, \dots, \hat{a}_{d_j}, \dots, \hat{a}_1, \hat{a}_2, \dots, \hat{a}_n]^T \quad (\text{A1})$$

$$\hat{a}^\dagger = [\hat{a}_{d_1}^\dagger, \hat{a}_{d_2}^\dagger, \dots, \hat{a}_{d_j}^\dagger, \dots, \hat{a}_1^\dagger, \hat{a}_2^\dagger, \dots, \hat{a}_n^\dagger]^T \quad (\text{A2})$$

A general quadratic Hamiltonian like Eq.(11) can be written as

$$\hat{H}^H = (\hat{a}^\dagger)^T w(t) \hat{a} + (\hat{a}^\dagger)^T m(t) \hat{a}^\dagger + \hat{a}^T m(t)^H \hat{a} \quad (\text{A3})$$

where $w(t)$ and $m(t)$ are the coefficient matrices, and $m(t)^H$ is the conjugate transpose of $m(t)$, $m(t)^H = m(t)^{T*}$. Combine Eqn.(15) and (A3), one obtains the matrix form of $F(t)$ as follows

$$F(t) = \begin{bmatrix} A(t) & Ct \\ C(t)^H & B(t) \end{bmatrix} \quad (\text{A4})$$

where

$$A(t) = \frac{1}{2}(w(t) + m(t) + m(t)^H) \quad (\text{A5})$$

$$A(t) = \frac{1}{2}(w(t) - m(t) - m(t)^H) \quad (\text{A6})$$

$$A(t) = \frac{1}{2}(w(t) - m(t) + m(t)^H) \quad (\text{A7})$$

Appendix B: Causality analysis on UV cutoff

Before we go further to discuss quantum correlation between the detectors we should discuss the cutoffs we adopt. A cavity length naturally limits the lowest energy of the mode with the longest wavelength. A single mode approximation in the Unruh-Dewitt model can lead to unphysical results such as the broken causality. [38] For the convergent result, one should consider infinitely many modes. But this is not possible for practical calculations, so a UV cutoff is necessary. How do we know whether the UV cutoff is reasonable? The appropriate cutoff was selected based on whether the accelerator strictly produces the corresponding Unruh temperature in [28]. A larger cutoff corresponds to an exact Unruh effect $T = a/2\pi$. In our study, we focus on checking on the correlation between the bipartite detectors in acceleration and in thermal field. It is difficult to find the appropriate cutoff working for the individual detector which can still hold for the bipartite detectors. In this situation, we consider another criterion which is based on whether the causality is broken. It has been shown that the finite number of modes can lead to a superluminal signaling. Nevertheless, it is possible to find an effective model with a finite number of modes such that acausal signaling does not appear within the required arbitrarily high time precision. [23] Consider the following setup, the detector 1 and the detector 2 are stationary and separated at a distance in a cavity. The detector 1 is at the vacuum state and the detector 2 is at the vacuum or the excited state. We want to examine how long it takes the detector 1 to observe the effects of the detector 2 via propagating the excitation in the field. The excitation probability of the detector 1 is given as [39]

$$p = 1 - \frac{2}{\sqrt{\det(\sigma_{d_1}) + \text{Tr}(\sigma_{d_1}) + 1}} \quad (\text{B1})$$

We will furthermore take the highly excited state of detector 2 to be specifically a single mode squeezed state with a covariance matrix of the form.

$$\sigma_{d_2} = \begin{bmatrix} e^{2r} & 0 \\ 0 & e^{-2r} \end{bmatrix} \quad (\text{B2})$$

where r is the squeezing parameter. In Figure 9(a) 9(b), we plot the excitation probability of the detector 1 as a function of t/t_c . We show the results including 7 and 10

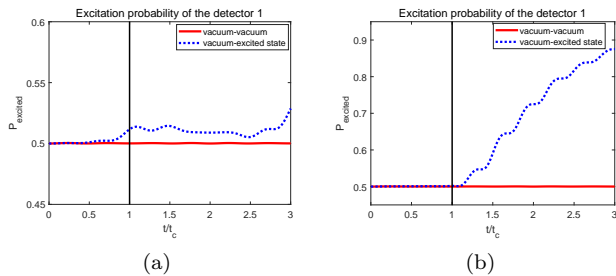


FIG. 9. Excitation probability as a function of t/t_c of an inertial detector (detector 1) in the presence of another in a highly excited state (detector 2) considering (a) 7 modes and (b) 10 modes. The vertical line in the Figure 9(a) 9(b) represents the moment in time t/t_c at which the two detectors come into causal contact. In each of the figures the blue dashed curve is the excitation probability for the detector 1 when the detector 2 is initially in its vacuum state, whereas for the solid (red) curve we initialize detector 2 in a squeezed state with squeezing parameter $r = 5$. The blue dashed line deviates from red solid line in case (a) while the blue conforms to the red in case (b) before the two detectors come into causal contact. Notably, there are also certain slight deviations in the case (b). The parameter values are $L = 4\pi$, $\lambda = 0.05$ and $\Omega = 3/2$. The detector 1 is at π and the detector 2 is at 3π . The periodic boundary conditions are used here.

field modes. The vertical line in the Figure represents the moment t/t_c at which the two detectors come into causal contact. In each of the plots the blue dashed curve is the excitation probability for detector 1 when detector 2 is initially in its vacuum state. For the solid (red) curve we initialize the detector 2 in a squeezed state with squeezing parameter $r = 5$. Increased excitations in the detector 1 caused by the propagating field quanta emitted from the squeezed detector 2 is observed as we expected. We also observe that if one does not use enough field modes, then the additional excitation occurs before the two detectors are in causal contact as in Figure 9(a). It is only when including enough field modes that we find the two curves start to diverge at t/t_c , as in Figure 9(b). This shows the place when they start to have the mutual influence. Notably, there are also certain slight deviations in the Figure 9(b). Increasing the number of mode we adopt, the deviation before causal contact becomes extremely small until the precision specified. Consider-

ing that physical UV and IR cutoffs must guarantee the causality, we examine the causality to determine whether a mode number is appropriate or not.

Appendix C: The nonequilibrium quantum correlations in the coordinate time

We plot the figures of the quantum correlations with respect to the coordinate time and the acceleration difference in figure 10(a)~ 10(c). The entanglement decreases but the mutual information (discord) is amplified by the

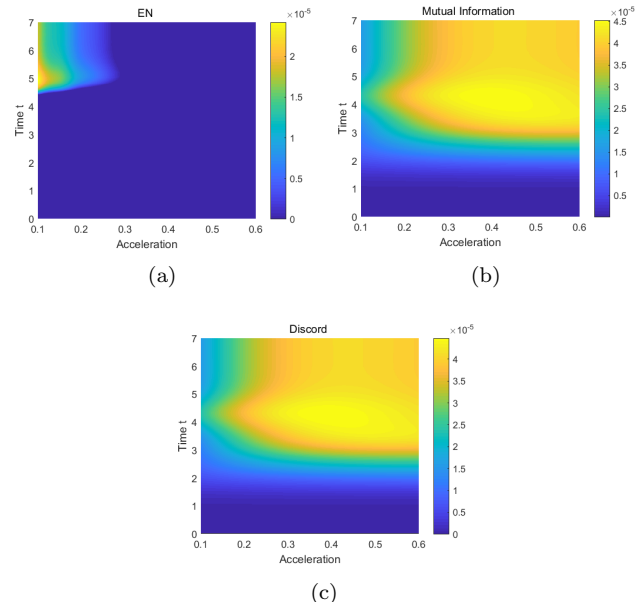


FIG. 10. Figure 10(a) 10(b) 10(c) describes how E_N , mutual information and quantum discord varies with respect to the acceleration difference and the coordinate time t . Alice stays at a lower acceleration 0.1 and Bob has a larger acceleration starting from 0.1. All the parameters are the same as those in Figure (1a) (1b). Here we can see significant redshift effect in the coordinate time, and the period is elongated.

higher acceleration difference. Here we can see significant redshift effects in the coordinate time, while the period is elongated.

[1] Nielsen Michael A., Chuang Isaac L., *Quantum Computation and Quantum Information: 10th Anniversary Edition*, (Cambridge University Press, 2011).
 [2] Einstein A., Podolsky B., Rosen N., *Can Quantum-Mechanical Description of Physical Reality Be Considered Complete?*, Phys. Rev. **47** 777-780 (1935).
 [3] Horodecki R., Horodecki P., Horodecki M., et al, *Quantum entanglement*, Rev. Mod. Phys. **81** 865-942 (2009).

[4] Belavkin V. P., Ohya M., *Entanglement, Quantum Entropy and Mutual Information*, Proceedings of The Royal Society A Mathematical Physical and Engineering Sciences **458**209-231(2002).
 [5] H. Ollivier and W. H. Zurek, *Quantum Discord: A Measure of the Quantumness of Correlations*, Phys. Rev. Lett. **88** 017901(2001).
 [6] Adesso G., Fuentes Schuller I., Ericsson M., *Continuous variable entanglement sharing in non-inertial frames*,

- Phys. Rev. A **76**(6)62112-62112 (2007).
- [7] Fuentes Schuller I., Mann R. B., *Alice falls into a black hole: Entanglement in non-inertial frames*, Phys. Rev. Lett. **95**(12) 120404 (2004).
- [8] Alsing P. M., Fuentes-Schuller I., Mann R. B., et al, *Entanglement of Dirac fields in non-inertial frames*, Phys. Rev. A **74**(3) 396-401 (2006).
- [9] Ball J. L., Fuentes-Schuller I., Schuller F. P., *Entanglement in an expanding spacetime*, Physics Letters A **359**(6) 550-554 (2006).
- [10] Ling Y., He S., Qiu W., et al, *Quantum entanglement of electromagnetic field in non-inertial reference frames*, Journal of Physics A Mathematical and Theoretical **65**(30) 9025-9032 (2007).
- [11] E. Martin Martinez, Menicucci N. C., *Cosmological quantum entanglement*, Class. Quantum Grav. **29**(22) 224003 (2012).
- [12] E. Martin Martinez, Menicucci N. C., *Entanglement in curved spacetimes and cosmology*, Class. Quantum Grav. **31**(21) (2014) .
- [13] Unruh, W. G., *Notes on black hole evaporation*, Phys. Rev.D **14**(4) 870-892 (1976).
- [14] Hawking S. W., *Particle Creation by Black Holes*, Communications in Mathematical Physics **43** 199-220 (1975).
- [15] Schweber, Silvan S. and Polkinghorne, J. C., *An Introduction to Relativistic Quantum Field Theory*, Physics Today **15**(3) (1961).
- [16] Bruschi D. E., Louko J., E. Martin Martinez, et al, *The Unruh effect in quantum information beyond the single-mode approximation*, Phys. Rev. A **82** 042332 (2010).
- [17] B. DeWitt, *General Relativity; an Einstein Centenary Survey*, (Cambridge University Press, Cambridge, UK, 1980).
- [18] Crispino L. C. B., Higuchi A., Matsas G. E. A., *The Unruh effect and its applications*, Rev. Mod. Phys. **80**(3) 787-838 (1975).
- [19] E. Martin Martinez, Brown E. G., Donnelly W., et al, *Sustainable entanglement production from a quantum field*, Phys. Rev. A **88**(5) 11592-11604(2013).
- [20] Allison Sachs, Robert B. Mann, E. Martin Martinez, *Entanglement harvesting and divergences in quadratic Unruh-DeWitt detector pairs*, Phys. Rev.D **96**(8) 080512 (2017).
- [21] Lin S. Y., Chou C. H., Hu B. L., *Disentanglement of two harmonic oscillators in relativistic motion*, Phys. Rev. D **78**(12) 667-670 (2008).
- [22] Lin S. Y., Hu B. L., *Entanglement creation between two causally-disconnected objects*, Phys. Rev. D **81**(4) 389-398 (2009).
- [23] Brown E. G., E. Martin Martinez, Menicucci N. C., et al , *Detectors for probing relativistic quantum physics beyond perturbation theory*, Phys. Rev. D **87**(8) 084062 (2013).
- [24] Brown E. G., Eric G., *Thermal amplification of field correlation harvesting*, Phys. Rev. A **88**(6) 062336 (2013).
- [25] Adesso G., Ragy S., Lee A. R., *Continuous variable quantum information: Gaussian states and beyond*, Open Systems and Information Dynamics **21**(01n02) 1440001 (2014).
- [26] Adesso G., Illuminati F., Donnelly W., et al, *Entanglement in continuous variable systems: Recent advances and current perspectives*, Journal of Physics A General Physics **40**(28) 7821-7880 (2007).
- [27] Adesso G., Datta A., *Quantum versus classical correlations in Gaussian states*, Phys. Rev. Lett. **105**(3) 030501 (2010).
- [28] Vriend S., Grimmer D., E. Martin Martinez, *The Unruh effect in slow motion*, arXiv:2011.08223 (2020).
- [29] Wilson G. Brenna, Eric G. Brown, Robert B. Mann, and E. Martin Martinez, *Universality and thermalization in the Unruh effect*, Phys. Rev. D **88** 064031 (2013).
- [30] Bellomo B., Franco R. L., Compagno G., *Non-Markovian effects on the dynamics of entanglement*, Phys. Rev. Lett. **99**(16) 160502 (2007).
- [31] Heinz-Peter Breuer, Elsi-Mari Laine, Jyrki Piilo, and Bassano Vacchini, *Non-Markovian dynamics in open quantum systems*, Rev. Mod. Phys. **88** 021002 (2016).
- [32] Breuer H. P., Petruccione F., *The Theory of Open Quantum Systems*, (Oxford University Press, 2006).
- [33] Fanchini F. F., Cornelio M. F., De Oliveira M. C., et al, *Conservation law for distributed entanglement of formation and quantum discord*, Phys. Rev. A **84**(1) 012313 (2010).
- [34] Madhok V., Gupta V., Trottier D. A., et al, *Signatures of chaos in the dynamics of quantum discord*, Phys. Rev. E **91**(3) 032906 (2015).
- [35] Grant Salton, Robert B. Mann and Nicolas C. Menicucci, *Acceleration-assisted entanglement harvesting and rangefinding*, New J. Phys **17** 035001 (2015).
- [36] Birrell N. D., Davies P., *Quantum Fields in Curved Space*,(Cambridge University Press, 1982).
- [37] Zhihai Wang, Wei Wu, and Jin Wang, *Steady-state entanglement and coherence of two coupled qubits in equilibrium and nonequilibrium environments*, Phys. Rev. A **99** 042320 (2019)
- [38] Dionigi M. T. Benincasa, Leron Borsten1, Michel Buck1 and Fay Dowker, *Quantum information processing and relativistic quantum fields*, Class. Quantum Grav. **31** 075007 (2014)
- [39] V. V. Dodonov, O. V. Man'ko, and V. I. Man'ko, *Photon distribution for one-mode mixed light with a generic Gaussian Wigner function*, Phys. Rev. A **49** 2993 (1994)